TRANSPORT
ISSN 1648-4142 / eISSN 1648-3480
2022 Volume 37 Issue 1: 37–50
https://doi.org/10.3846/transport.2022.16919

DEEP NEURAL NETWORK BASED DATA-DRIVEN VIRTUAL SENSOR IN VEHICLE SEMI-ACTIVE SUSPENSION REAL-TIME CONTROL

Paulius KOJIS, Eldar ŠABANOVIČ*, Viktor SKRICKIJ

Transport and Logistics Competence Centre, Vilnius Gediminas Technical University, Lithuania

Submitted 23 February 2022; resubmitted 26 April 2022; accepted 30 April 2022

Abstract. This research presents a data-driven Neural Network (NN)-based Virtual Sensor (VS) that estimates vehicles' Unsprung Mass (UM) vertical velocity in real-time. UM vertical velocity is an input parameter used to control a vehicle's semi-active suspension. The extensive simulation-based dataset covering 95 scenarios was created and used to obtain training, validation and testing data for Deep Neural Network (DNN). The simulations have been performed with an experimentally validated full vehicle model using software for advanced vehicle dynamics simulation. VS was developed and tested, taking into account the Root Mean Square (RMS) of Sprung Mass (SM) acceleration as a comfort metric. The RMS was calculated for two cases: using actual UM velocity and estimations from the VS as input to the suspension controller. The comparison shows that RMS change is less than the difference threshold that vehicle occupants could perceive. The achieved result indicates the great potential of using the proposed VS in place of the physical sensor in vehicles.

Keywords: virtual sensor, real-time, semi-active suspension, vehicle dynamics, deep neural network, deep learning.

Notations

ANN – artificial NN;
CDC – continuous damping control;
CNN – convolution NN;
DCC – dynamic chassis control;
DNN – deep NN;
ECU – electronic control unit;
ESC – electronic stability control;
FC – fully connected;
FL – front left;
FR – front right;
GA – genetic algorithm;
IMU – inertial measurement unit;
LIDAR – light detection and ranging;
LQR – linear quadratic regulator;
LReLU – leaky rectified linear unit;
MEMS – microelectromechanical sensors;
MPC – model predictive control;
MR – magnetorheological;
NN – neural network;
PID – proportional integral derivative;
RL – rear left;
RMS – root mean square;
RMSE – RMS error;
RR – rear right;
SH-ADD – *Skyhook* acceleration driven damper;
SM – sprung mass;
SMC – sliding mode control;
SUV – sport utility vehicle;
UM – unsprung mass;
VS – virtual sensor.

Introduction

Recent progress in automated driving reduces drivers' involvement in the driving process. In the near future, the occupant will be able to carry out various activities, e.g., working, surfing the internet, reading while the vehicle is moving. A new comfort level must be achieved in such vehicles. As a result, suspension architecture should be reviewed, and new solutions for active suspensions and their components are needed.

Vehicle suspension maintains the correct vehicle body orientation, provides good ride comfort and ensures desirable handling and safety capabilities (Skrickij *et al.* 2018; Cao *et al.* 2011). The suspension consists of rigid links, stiffness and damping elements and, optionally, controlla-

*Corresponding author. E-mail: *eldar.sabanovic@vilniustech.lt*

ble actuators. Based on its structure and possibility of control, it can be classified as passive, adaptive, semi-active, and active.

The passive suspension system consists of constant stiffness springs and shock absorbers with a fixed damping coefficient. The selection of the optimal damping and stiffness levels requires a compromise between vehicle handling and ride comfort (Yatak, Şahin 2021).

The adaptive suspension system realises a slow (<1 Hz) variation of the spring and the damper characteristics. The variation is scheduled: it may be presented before the actual driving or may differ according to the vehicle's velocity to lower its centre of mass to ensure better handling. The energy consumption of such a system is significantly lower compared to the active suspension (Koch 2011).

Semi-active suspensions offer the possibility for the adjustment of damper characteristics in real-time. The main attribute of semi-active systems is that the force generated by the actuator, usually a damper with variable force–velocity characteristics, depends on the direction of relative motion (Koch 2011). This is considered a limitation because this suspension type cannot control the vehicle's ride height, roll, or pitch angle (Theunissen *et al.* 2021). On the other hand, semi-active suspension can operate within the low power consumption range due to the indirect generation of the actuator force. All of the power supply is only required to activate auxiliary components of suspension (Theunissen *et al.* 2021). From the constructive point of view, semi-active suspension can be implemented using hydraulic shock absorbers, MR and electromagnetic dampers (Soliman, Kaldas 2021). MR dampers utilise magnetic oils whose viscosity can be affected by electromagnetic fields. When the magnetic coil is activated, MR fluid particles align with the direction of the magnetic flux, thus increasing the damping properties (Ghoniem *et al.* 2020). The hydraulic shock absorbers utilise aperture related fluid flow control. This is usually implemented using a valve with the variable orifice or bypass valve with the solenoid. The dissipation level is varied by changing the cross-section of the opening between the damper chambers (Savitski *et al.* 2017). The electromagnetic damper's operating principle is based on the interaction between the moving coil and the magnetic field of a permanent magnet or electromagnet to provide a damping effect. The damping level can be varied by altering the external resistance or the strength of the magnetic field. In the case of a damper coil short circuit or connection to an external resistor, the device performs as a passive shock absorber. The electromagnetic damper's main drawback is its high cost (Soliman, Kaldas 2021).

Active suspension can be implemented using electromechanical, electromagnetic, and electrohydraulic actuators. The controllable actuators are installed between the UM and the SM. Contrary to semi-active suspension, the direction of the actuator generated force is independent of the relative actuator motion, which is beneficial for performance. This advantage compensates for the vehicle body's roll, pitch and heave motions and controls the ride height (Theunissen *et al.* 2021). Although the active suspension provides better performance in a wide variety of road conditions and terrains it is very complex, consumes high amounts of energy and is still quite expensive to commercialise and utilise in economy class vehicles (Ghoniem *et al.* 2020).

Nevertheless, some suspension actuators can also recuperate energy from road oscillations contributing to the better energy efficiency of the system (Sathishkumar *et al.* 2021). In the electrohydraulic actuator approach, system performance strongly depends on the characteristics of its components. Higher flow of hydraulic pump allow achieving better actuator force–velocity properties. A hydraulic accumulator ensures the required fluid pressure and/or flow rate. Thus, the active valves can control the damping levels and generate additional force (Vandersmissen *et al.* 2012). In comparison, electromechanical actuators may include an electric motor and a mechanical system to convert the angular displacement of the rotor into a linear actuator displacement. It must be noted that electrohydraulic design tends to have lower system bandwidth compared to one with electromechanical actuators. Nevertheless, benefits in control lead to higher energy consumption. Thus, choosing between electromechanical and electrohydraulic approaches leads to a trade-off between energy consumption and performance (Savitski *et al.* 2017).

Controlled suspensions use input data from the acceleration sensors placed on the SM and the suspension displacement sensors installed between the vehicle body and the suspension's lower control arms. Sometimes additional acceleration sensors are placed on UM as well. Additional inputs are commonly used for control, such as steering wheel angle, vehicle speed, brake pressure, and others (Soliman, Kaldas 2021).

The manufacturers have developed various suspension systems. ZF Sachs AG has developed CDC suspension. It uses six strategically placed accelerometers in the vehicle to detect wheel and body movement. An ECU then processes that information, communicates with the brake, steering, engine, and ESC modules and calculates the necessary damping force (Soliman, Kaldas 2021). Bilstein developed the *DampTronic*® sky system. Using the data from the acceleration and suspension displacement sensors, the suspension control module individually adapts the damping forces for each wheel (Soliman, Kaldas 2021). *Volkswagen AG* has developed the DCC system based on semi-active dampers. The DCC system uses three accelerometers placed on the vehicle body and three suspension displacement sensors (Soliman, Kaldas 2021). *Ford Motor Company* has developed a semi-active suspension system. The *Ford* system uses four height sensors to measure the relative displacement between the vehicle body and wheels (Soliman, Kaldas 2021). From these examples, it is clear that various combinations of accelerometers and displacement sensors dominate in the commercially available controlled suspensions.

With the appearance of semi-active and active suspension systems, various controllers with different control strategies emerged. A proper control algorithm must be implemented to ensure suspension performance for ride comfort and handling (Ghoniem *et al.* 2020).

The most common suspension control strategies depend on rule-based discontinuous or continuous damping factor switching (Floreán-Aquino *et al.* 2021). Some key examples of such strategies are *Groundhook* and *Skyhook* for vehicle handling and comfort accordingly. Furthermore, the combinations of these two, called hybrid and mixed SH-ADD control, were created to provide both comfort and handling (Savaresi *et al.* 2010; Qin *et al.* 2018).

In addition, the classical control includes a PID controller. PID ensures a controlled response by applying tunable gains in vehicle suspension application. It automatically applies certain corrections to reach the desired response based on the actual system and its feedback. For best PID performance, gain parameters require adaptive tuning. That can be implemented using fuzzy logic and function optimisation based tuning (Jain *et al.* 2020; Marques, Reynoso-Meza 2020). Furthermore, the SMC strategy drives a controlled system onto a particular surface, defined by boundary conditions and desired states. This feedback controller impulses the system to reach the sliding surface within a finite time and make it toggle between two phases, either on and off or reverse and forward. The control input is sustained when the system is finally at the sliding surface (Al-Ashmori, Wang 2020). In practice, SMC is defined by governing switching rules, weighted matrices, vehicle mathematical model, driven polynomial sliding surface and suspension performance index. The performance index is mostly based on the quadratic optimal control theory to minimise absolute body vertical acceleration, dynamic wheel loads, and suspension deflection (Zhou *et al.* 2018).

Moreover, Savitski *et al.* (2017) proposed a hierarchical control architecture to reduce the vehicle's vertical, pitch and roll rates. The proposed control strategy applies the integral SMC approach and optimal distribution of virtual demand between four semi-active shock absorbers. If not used in conjunction with different methods, these conventional techniques contain some drawbacks, such as chattering in high frequencies and reduced bandwidth. That limits the capacity for improving passenger comfort, simultaneously road holding. In addition, not all of the reviewed control strategies contain predefined control laws. Therefore, applying a specific method to the real suspension system may be complex (Floreán-Aquino *et al.* 2021).

Intelligent suspension control includes the following methods: fuzzy logic, MPC and ANN. The fuzzy logic strategies assign the damping coefficient without a precisely constructed mathematical model for the system control. A rule-based algorithm can assign the required damping for certain road excitation (Ghoniem *et al.* 2020). MPC utilises vehicle suspension model-based optimisation in a finite time domain. MPC solves the optimisation task to predict the optimal control variables from the current and preferred systems at each sampling period. After that, the controller corrects the future output at the next moment according to the error between the system output and the predicted output to realise the closed-loop of the overall optimisation (Jiang *et al.* 2021). Zheng *et al.* (2021) proposed nonlinear MPC for enhancing motion comfort, and the solution led to a significant reduction of the lateral acceleration sensed by the passenger over a vehicle with passive suspensions by 46.5%

Furthermore, the ANN controllers can assign the needed damping forces in abnormal conditions like ageing and deterioration of the damper. The existing system's response is monitored and compared with the suspension design parameters in such a strategy. The ANN controller generates new corrected tuning signals to the damper (Savaresi *et al.* 2019). The ANN controllers often replace the conventional controllers by investigating the conventional systems and using their data to learn control patterns. A good example that motivates the use of ANN as the controller is research performed by Konoiko *et al.* (2019). An ANN was trained by the optimal PID and surpassed it under parameter uncertainties. ANN is used in combination with traditional controllers, including the SMC, PID and LQR, to enhance the controller performance and other tasks such as determination of the road roughness, an indication of damper deterioration or the tuning of gain (Fares, Bani Younes 2020).

The latest control strategies are categorised as preview-based and learning-based methods. Road profile is not an unknown disturbance in preview-based control but is a measured or estimated external input. Preview control formulations are either based on the road irregularities at a single point or a set of discrete points. Typically, the information covers the range from the current longitudinal coordinate of the vehicle to a predicted future position of the wheel. In practice, preview-based algorithms are implemented using the "look-ahead" sensor (e.g., LIDAR camera and radar) or the wheelbase preview assumption (Theunissen *et al.* 2021). In fact, with the road preview, the suspension actuator can proactively respond to a road excitation before actually reaching it. Therefore, reducing both SM acceleration and suspension deflection. Learning-based suspension controllers use knowledge-based systems and statistical learning methods. These suspension controllers can learn from the environment and adapt the model parameters accordingly. Moreover, this approach enables simultaneous road classification and vehicle suspension control. Learning systems can quantify model uncertainties appropriately. Soft computing-based learning methods represent GA, ANN, MPC and various combinations of fuzzy controllers. On the other hand, statistical computing-based learning methods use parametric statistical regression models or probabilistic methods (Mozaffari *et al.* 2019). Described control strategies can significantly increase ride comfort and handling but re-

quire high computational power; therefore, may be challenging to implement in real-time applications and possess a considerable number of tuning parameters to define.

As stated before, control incorporation into the suspension requires sensors to collect data. Different types of sensors introduce complexity to the system. There are added production and maintenance costs related to the use of displacement sensors. These sensors measure UM mass displacement in reference to SM mass. In addition, UM mass velocity in reference to SM mass is estimated based on these measurements. In contrary to acceleration sensors, which are MEMS mounted on SM mass and did not require maintenance as they measure acceleration in a non-contact way, displacement sensors are usually mechanical devices attached between SM and UM masses on four sides of the vehicle. Therefore, they are prone to wear and may require frequent changes. In addition, they add cost to the vehicle and additional mass. Many investigations of virtual sensing have been published (Acosta *et al.* 2017; Sun *et al.* 2017; Ahamed, Duraiswamy 2019; Martin *et al.* 2021). The VS combines existing signals from other on-board physical sensors to approximate the system's state and create virtual signals of non-measured values (Li *et al.* 2011). The use of VSs instead of physical ones solves the problem of cost and maintenance. This is possible if the VS can be implemented in current on-board computers. Implementation of VSs in various systems provides many advantages. One of several is the more forthright usage of sensors in compact areas: hydraulic systems, wheel carriers, etc. Technology offers a possibility to measure unmeasurable or complex values such as performance or efficiency indexes. By using VS system, physical parts count decreases, and overall reliability increases. Implementation requires additional development costs but reduces repetitive maintenance intervals and costs (Li *et al.* 2011). The possibility of diagnosing and predicting the system's state in advance emerges (Mattera *et al.* 2018). VS measures variables without adding the corresponding physical errors (Choi, Yoon 2020). It interprets data and finds hidden relationships or correlations between variables. Various online identification algorithms can update VS when system parameters change (Khatibisepehr *et al.* 2013).

VS can be model-based or data-driven. In model-based VS, connections between inputs and outputs are described by mathematical equations, which make up a model (Sun *et al.* 2017). The creation of a model-based on physical properties requires high competencies and skills. Often, Kalman filters with vehicle models to update estimations are used (Pletschen, Badur 2014). The more accurate the model is, the more accurate the prediction will be; any change in vehicle parameter will require a change in the model. This must be considered during the sensor development stage, and will require a more complex algorithm that may use more computational power (Omrane *et al.* 2015). The strengths of the model-based VS are predictability and low requirements for experimental data. The main weakness of the model-based approach is that the accuracy of VS depends on the complexity of the model, and it depends on the expertise of the model's creators. Besides that, there are not many established UM vertical velocity estimation models. Otherwise, data-driven VS based on machine learning technics require little prior knowledge about the system but much data to be recorded. VS may fail to estimate the system's state accurately if low dynamic data content is provided. Therefore, an insignificant error can generate a significant drift in the estimated signals (Acosta *et al.* 2017). If the vehicle is operating in a wide range and, as a result, measurement values are changing in a wide range, the VS must scale accordingly to deliver satisfactory performance. The dataset should cover the full range of possible input and output values to achieve that. In the case of the VS, physical sensors that are not possible or too expensive to use in real-life conditions can be used to collect huge amounts of data for the development of data-driven VS (Li *et al.* 2011; Sun *et al.* 2017). The main weakness of data-driven VS is that it is a requirement for a huge dataset. It can be manageable, and performance can achieve and surpass model-based approaches where a complex model is required. The main strength of the data-driven VS is the ability to model complex relations between input and output data based on collected datasets without prior knowledge of the system; therefore, results will not depend on the competence and expertise level of the creators. Recently, hybrid model-based and data-driven approaches appear that are promising to provide benefits of both (Son *et al.* 2020).

There are several publications on VSs implementations in various vehicle systems. In the review paper (Zaharia, Clenci 2013), the authors highlight areas in the automotive industry where VSs are applied: (1) passenger thermal comfort observation and regulation; (2) tire pressure monitoring system; (3) powertrain applications. VSs are applied in active noise cancellation to lower the noises of the truck and car engines (Ahamed, Duraiswamy 2019). Vehicle yaw rate estimation using a VS is presented in the paper by Kahraman *et al.* (2010). A relative suspension velocity estimation is carried out in the strategy proposed by Jeong and Choi (2019). The method consists of mathematical modelling and direct measurements provided by an IMU. In Milanese *et al.* (2007), the authors used the direct VS design technique to estimate the relative vertical displacement and velocity between chassis and wheel. Pletschen and Badur (2014) provided VS for suspension state estimation based on Kalman Filter and Takagi–Sugeno modelling. In Viehweger *et al.* (2020), authors estimate tire forces using NN-based VS. In Kim *et al.* (2021), authors estimate unknown road profiles using NN-based VS. Earlier, in Šabanovič *et al.* (2021), the authors proved that NN-based VS could be used estimate UM vertical velocity for a vehicle with passive suspension. Nevertheless, the VS was not used on real or simulated vehicles with a controlled suspension system. NN models and especially DNN have already proved the capability to learn the signal

features and provide very good results for regression tasks simultaneously, especially in the supervised learning approach. Therefore, DNN selected the proposed data-driven VS out of all possible artificial intelligence methods.

It was found that there is no research about change in comfort level metrics because of the use of VS for vertical UM velocity instead of a physical sensor, this paper targets this issue. Therefore, the most common suspension control strategy – *Skyhook*, was implemented in the vehicle to test the impact of the VS. There, the hypothesis is raised that VS will impact comfort level less than can be felt by the occupant. This paper presents a comparison between comfort metric RMS estimated for running with the same control algorithm while using UM vertical velocities data directly from simulation and VS.

The developed sensor is integrated and tested on a simulation platform using a high-fidelity SUV model for the first time. The observed changes in the RMS metric of comfort level are evaluated based on the human sensitivity threshold and showed that in the majority of test cases, change in the RMS metric would be less than a threshold value.

In current section, an introduction and literature review is presented. In Section 1, the theoretical background, including the vehicle mathematical model and semi-active suspension control strategy. A real-time data-driven VS and a dataset are presented. In Section 2, a comparison of conventional passive suspension and semi-active is provided when driving on different surfaces. The VS is integrated into the mathematical model, and the output is used for real-time control of a vehicle's semi-active suspension. The effectiveness of the proposed solution is evaluated. In last section, conclusions and future plans are presented.

1. Theoretical background

This Section describes the materials and methods used for research. In Figure 1, research at a glance is presented. The aim is to use a virtual DNN-based, data-driven sensor for UM vertical velocity estimation instead of physical. A vehicle mathematical model with semi-active suspension is needed to test the idea. The structure of DNN used for the VS of vehicle UM vertical velocity estimation needs to be developed; it requires the development of the original dataset. The proposed system is evaluated by comparing SM vertical acceleration RMS to achieved by using the reference system.

As pictured in Figure 1, this research aims not to create a new control strategy for the suspension. Rather, evaluate VS impact on the passenger comfort level and test it in a real-time suspension control application. Therefore, reference systems include simulated physical sensor data and the proposed system that uses VS to estimate vertical velocity. In both systems, measurements from the sensors are fed into the same *Skyhook* control algorithm. Afterwards, the impact on SM vertical acceleration is estimated by the difference in the calculated RMS metric.

1.1. Vehicle mathematical model

The vehicle mathematical model was developed on the *IPG CarMaker* simulation platform (*https://ipg-automotive.com/en/products-solutions/software/carmaker*) using a high-fidelity SUV model; its dynamic model is presented in Figure 2. The model has been parametrised based on mass-inertia parameters, suspension kinematics and compliance. The *Delft-tire* model was validated using test bench testing. The vehicle model has been validated using field test data from the proving ground, as described by Šabanovič *et al.* (2021).

1.2. Strategy for vehicle semi-active suspension control with VS

As shown in the introduction section, many control strategies have been developed during the last years for suspension control. However, many original equipment manufacturers use rule-based techniques based on *Skyhook* control strategies and their modifications (Pellegrini 2012). The principle of this approach is to minimise disturbance effects that cause the vehicle body vertical oscillations.

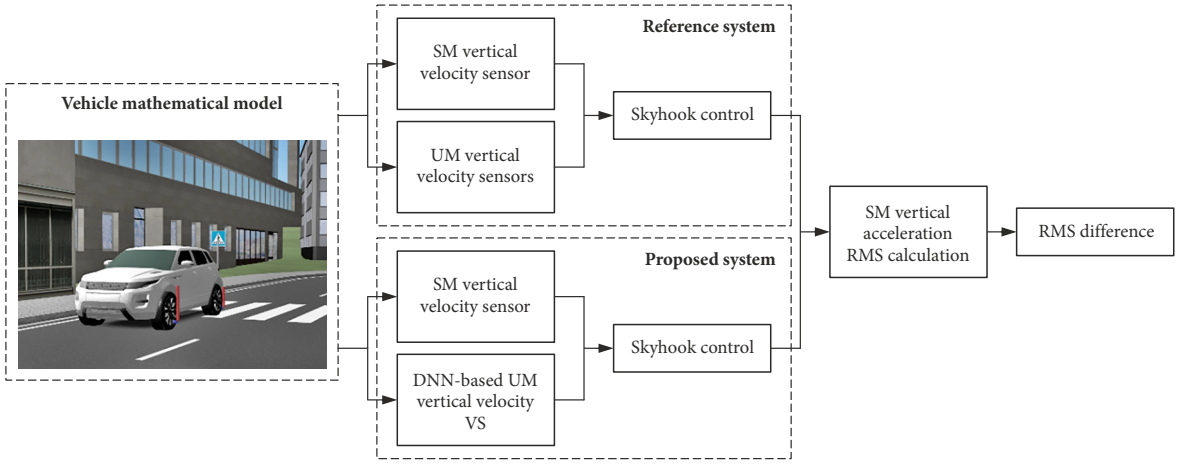

Figure 1. Research at a glance

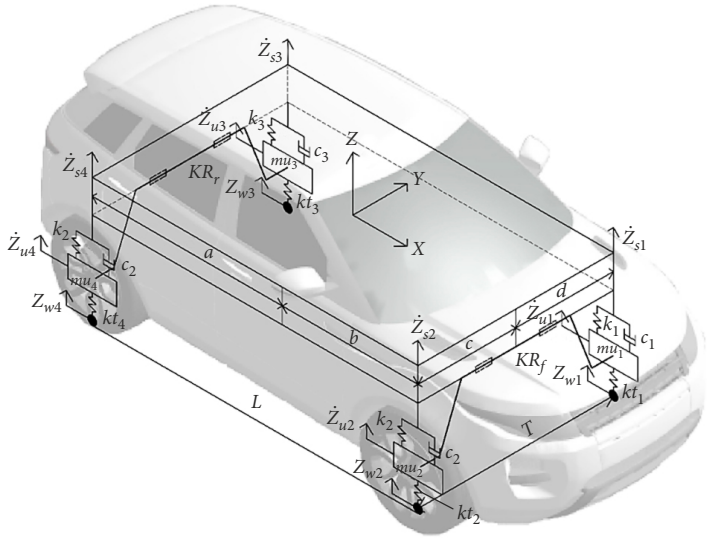

Figure 2. SUV dynamic model – modification of Šabanovič *et al.* (2021)

Based on the direction of motion of the vehicle body, the system's damping is either increased or reduced. Therefore, *Skyhook* control is easy to implement with information from a few sensors representing the vehicle state (Liu *et al.* 2019). Initially, the strategy attempted to simulate the virtual damper linkage with a fixed inertial system (the sky) to decouple the SM oscillations and increase passenger comfort.

In practice, it is implemented by changing the damping C_s of the shock absorber according to the difference between the SM–UM vertical velocities by using a logical rule (Savaresi *et al.* 2010):

$$C_s = \begin{cases} C_{\min}, & \text{if } \dot{Z}_b \cdot \left(\dot{Z}_b - \dot{Z}_w\right) \le 0; \\ C_{\max}, & \text{if } \dot{Z}_b \cdot \left(\dot{Z}_b - \dot{Z}_w\right) > 0, \end{cases} \tag{1}$$

where: $\dot{Z}_b$ – vertical vehicle body (SM) velocity; $\dot{Z}_w$ – vertical wheel (UM) velocity; $C_{\min}$, $C_{\max}$ – minimal and maximal damping values.

In the simulations, there was only high-level control considered. Therefore, no actuator mathematical modelling was performed, and no low-level control allocation was implemented.

1.3. Real-time data-driven VS

The proposed system uses DNN-based real-time data-driven VS. The DNN model used for VS was developed to achieve sufficient performance while running in less than 10 ms. The proposed 1D CNN model consists of 7 layers (Figure 3).

The proposed VS model accepts data as a 4D matrix, where dimension 1 is a number of signals; 2 is position in the time window; 3 (depth or channel) is always 1; 4 is sample number in batch (equals 1 during real-time processing). The 4D matrix is used as input to the 4D matrix input layer that is connected to the first convolutional layer.

The first convolutional layer does 1D convolution on each input signal in parallel, even if the 2D convolution function is used, as the convolutional kernel is made to take only a small portion of one input signal in the time window dimension. There are 128 kernels of 1×3 in the first layer, and the stride is 2. This layer's stride reduces the window size by a factor of 2. Each value in the resulting feature map is processed using the activation function. The LReLU function is used with a leakage coefficient of 0.1 as an activation function. This leakage multiplier was selected to allow at least minimal gradient calculation during deep learning-based on the backpropagation of error.

The second convolutional layer processes the result with 64 kernels of 1×4, stride 2 and the same activation function as in the first layer. This also reduces window size dimension by a factor of 2. This and previous convolutional layers extract local features of the signals. The convolution layer both learns what features should be extracted and let's detect the parts of the signal where the features are. In our case, location information is related to the sample location in the time window. This way convolutional layer looks into the time window of samples and extracts signals' features in time.

The next layer is made of fully connected neurons called FC. This layer has 64 neuron units, and each neuron is connected to each value in the input matrix. There each neuron makes perceptron operations (input multiplication by weights, summation, and activation). The activation function is the same as in previous layers. The result is processed using a random dropout layer.

Dropout is made with a probability of 0.5 for the value to withdraw. This layer is active only during training; it writes zeros to randomly selected values of the input vector and multiplies other values by the 1/probability. This way, the total sum of values remains unchanged. The results of dropout are used as input to the second FC layer. A probability level of 0.5 prevents the NN model from relying on any input value by forcing any further decisions

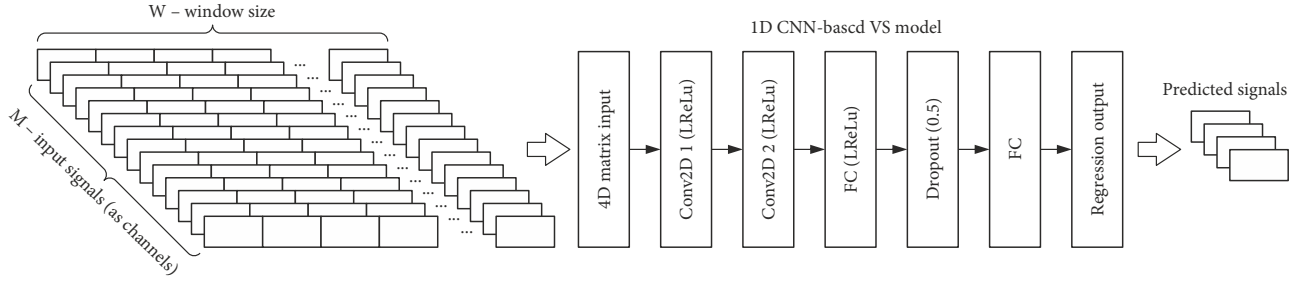

Figure 3. Structure of DNN-based VS with inputs and outputs

Table 1. Dataset description

Test name	Boundary conditions	Vehicle speeds
Trapezoidal road bumps tests (TFX^1VX^2)	hill ratios: i = 1:6…1:30; heights: h = 0.01…0.14 m; plateau lengths: L = 3…5 m	10, 15, 20, 25, 30, 35, 40, 45, 50, 55, 60 km/h
		Number of tests: 25
Sinusoidal waveform road profile tests ($SINX^1VX^2$)	amplitudes: A = 0.01…0.12 m; period lengths: P = 0.1…10 m	10, 15, 20, 25, 30, 35, 40, 45, 50, 55, 60 km/h
		Number of tests: 20
Checkered pattern of trapezoidal road bumps tests ($ChessX^1VX^2$)	hill ratios: i = 1:5…1:40; heights: h = 0.01…0.1 m; plateau lengths: L = 2…3 m; distances between bumps: K = 5…15 m	10, 15, 20, 25, 30, 35, 40, 45, 50, 55, 60 km/h
		Number of tests: 20
Road pits and inverse sinusoidal waveform road profile tests (HOX^1VX^2)	hill ratios: i = 1:6…1:24; depths: h = 0.01…0.09 m; plateau lengths: L = 3…5 m	10, 15, 20, 25, 30, 35, 40, 45, 50, 55, 60 km/h
	amplitudes: A = 0.01…0.09 m; period lengths: P = 0.1…5 m	10, 15, 20, 25, 30, 35, 40, 45, 50, 55, 60 km/h
		Number of tests: 30
		Total number of tests: 95

based on at least two input values. This also fosters better globalisation and reduces the probability of overfitting. On the other hand, lower values of probability would increase network bias and require more artificial neural units in layers prior to dropout to compensate. This would require more computational power; therefore, it was not considered.

The second FC layer has as many neurons as there are output signals. This layer decides which previous FC layer outputs should be combined using perceptron operations to get each output signal. Results of this layer are fed to regression output. Therefore, the network provides real-valued outputs that are an estimation of probably output signals. The output is a vector of 4 values; each value corresponds to the estimated UM relative vertical velocity of each suspension quarter: FL, FR, RL, and RR.

1.4. Dataset

The original dataset was created for VS development. It contains 95 tests, including different road profile parameters and vehicle driving speeds. A detailed description of the tests is presented in Table 1. Each of the tests was driven at five different velocities. Therefore, the lowest and the highest speed runs plus randomly selected one from the remaining three were used as the training data. The validation and testing scenarios there randomly picked from the remaining two runs. All in all, 57 tests were used for training, 19 for validation and 19 for testing.

The first group of tests includes various trapezoidal road bumps. Bump parameters variety is presented in Table 1 – values are taken from the LAKD (2010). The vehicle passed through seven trapezoidal road bumps during this test at a specified velocity. The second group includes sinusoidal road profiles (geometrical parameters and velocities are presented in Table 1). The third group includes trapezoidal road bumps placed in a checkered pattern. The vehicle in this scenario is subjected to road bumps only on one side, left or right, at a particular moment. The fourth group includes road pits (geometrical parameters and velocities presented in Table 1).

Dataset uses 14 parameters as inputs: SM accelerations in 3 directions (x, y, z), angular rates around these 3 axes, longitudinal vehicle velocity, 2 front wheels' steering angles and vehicle yaw angle, 4 angular velocities of the wheels. Parameters are commonly measured in the industry. The vertical velocities of four UM were used as an output.

To further explain the dataset variations, an abbreviation system is used. In Table 1, each test group is assigned an abbreviation (e.g., TFX^1VX^2, HOX^1VX^2). The numbers in the superscript indicates: 1 – modification of the track (A, B, C, D, E, F), 2 – vehicle speeds. Different boundary conditions define track modification, and vehicle speeds are listed in Table 1. Therefore, in Tables 2–4, an abbreviation system is used in the following section.

2. Results and their analysis

In this Section, a comparison of conventional passive suspension and semi-active is provided when driving on different surfaces. Accuracy of developed NN-based is presented. Finally, developed VS is integrated into the mathematical model, and output is used for real-time control of a vehicle's semi-active suspension. The effectiveness of the proposed solution is evaluated.

2.1. Vehicle dynamics with semi-active suspension

In this subsection effect of semi-active suspension on vehicle comfort is presented. Comfort can be expressed using the RMS value of SM acceleration in the vertical direction:

$$RMS = \sqrt{\frac{\sum_{i=1}^{n} a_{s\,i}^2}{n}}, \tag{2}$$

where: $a_{s\,i}$ is the numerical value of vertical acceleration at the sample i; n is the total number of samples.

Several road types were tested; the main results are presented in Table 2. It can be seen that the RMS of SM acceleration a_s decreased significantly, from 28.69 to 40.22%. However, it is well-known that *Skyhook* is used for comfort and negatively impacts vehicle handling. From the same table, it can be seen that the RMS of UM acceleration a_u increases in most cases. Analysis of normal tire force should be performed to get more information about handling. However, it is not part of this investigation.

Graphically SM acceleration is presented in Figure 4; it can be seen that using semi-active suspension accelerations is reduced. In addition, a faster oscillation setting time is achieved. Therefore, the passengers are exposed to smaller periods of overall vibration.

2.2. VS testing

After DNN training, results were tested using a testing dataset that contained 19 different cases. A comparison of some examples of actual and estimated UM velocities using VS is presented in Figure 5. It can be seen that the VS performs perfectly on trapezoidal road bumps and roads with pits; on sinusoidal roads, the difference is higher. To get numerical values of errors, RMSE can be calculated:

$$RMSE = \sqrt{\frac{\sum_{i=1}^{n} \left(v_{act\,i} - v_{virt\,i} \right)^2}{n}}, \tag{3}$$

where: $v_{act\,i}$ is the ith sample of actual UM velocity in the vertical direction; $v_{virt\,i}$ is the ith sample of vertical velocity estimated by designed DNN-based VS.

These velocities can be calculated for each wheel. RMSE values for the testing dataset are presented in Table 3. Values have the same units as the measured velocity. The RMSE indicates the mean amount of error between the expected value and the actual value. Therefore, it is suitable for objective evaluation, and the values are easy to interpret (Jierula *et al.* 2021). By analysing the three scenarios presented in Figure 5b stands out. The difference between the UM velocity from the actual sensor and the VS is high compared to the other two scenarios in Figure 5. Numerical values provided in Table 3 support the case that the sinusoidal waveform road profile and the one with a checkered pattern of trapezoidal road bumps produce the highest RMSE values. UM motion is very dynamic in these scenarios and the direction of velocity changes at high frequency. Therefore, the VS underestimates and overestimates the predicted output.

VS testing results show that an average RMSE achieved for all 19 scenarios was 0.062 m/s (Table 3). According to the scenarios, the most favourable and the worst VS performance were TFEV25 and ChessBV40/HOCV40, respectively. On the other hand, in some scenarios, the RSME values are higher; this is related to more dynamic conditions and transient state behaviour of the vehicle. This indicates that a more expanded dataset may contribute to reaching lower RMSE values. Nevertheless, the accumulated VS RMSE values are considered satisfactory since the curves of actual and predicted by VS are very similar (Figure 5). Based on that, it can be stated

Table 2. Comparison of reference passive suspension and semi-active suspension performance

Conditions	Passive suspension		Semi-active suspension		SM RMS decrease [%]
	RMS a_s [m/s^2]	RMS a_u [m/s^2]	RMS a_s [m/s^2]	RMS a_u [m/s^2]	
Trapezoidal road bumps (hill ratio i =1:19…1:24; height h = 0.07…0.09 m; vehicle velocity v = 40 km/h) (TFCV40)	1.078	2.435	0.717	3.621	40.22%
Sinusoidal road profile (amplitude A = 0.04…0.06 m; period length P = 2…3 m; vehicle velocity v = 50 km/h) (SINBV50)	1.959	10.65	1.407	9.682	32.79%
Unsymmetrical road bumps (hill ratio i = 1:25…1:35; height h = 0.06…0.08 m; distance between bumps K = 12 m; vehicle velocity v = 35 km/h) (ChessCV35)	0.534	1,439	0.400	2,819	28.69%

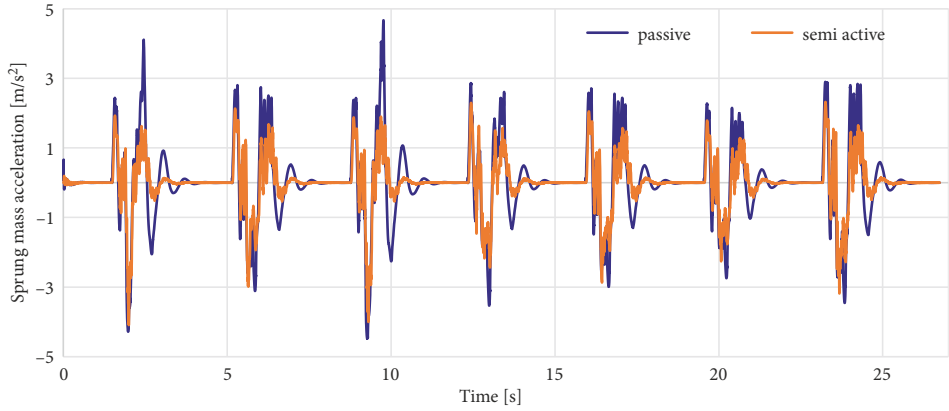

Figure 4. A suspension performance on trapezoidal road bumps, longitudinal vehicle velocity (40 km/h)

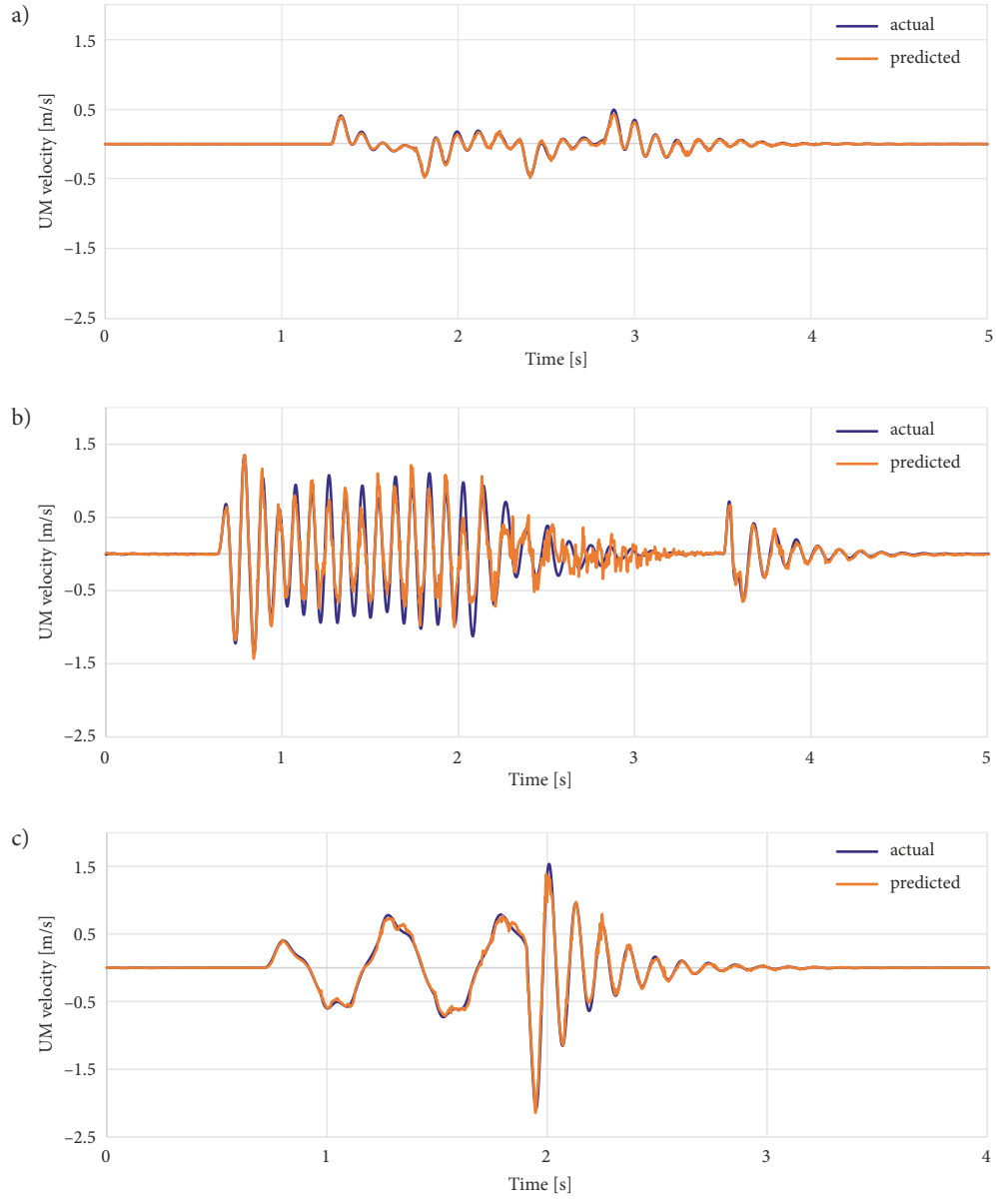

Figure 5. Signal repeatability with VS for specified wheel: a – trapezoidal road bumps test (25 km/h); b – sinusoidal road profile test (40 km/h); c – road with pits (20 km/h)

Table 3. RMSE achieved in testing scenarios for each wheel

Scenario	RMSE				
	FL	FR	RL	RR	Overall
TFAV50	0.037	0.037	0.048	0.048	0.042
TFBV25	0.026	0.025	0.057	0.057	0.041
TFCV30	0.028	0.028	0.062	0.062	0.045
TFDV40	0.031	0.031	0.072	0.072	0.051
TFEV25	0.016	0.016	0.038	0.038	0.027
SINAV40	0.102	0.104	0.099	0.098	0.101
SINBV40	0.071	0.073	0.089	0.089	0.081
SINCV30	0.062	0.062	0.107	0.110	0.085
SINDV25	0.020	0.020	0.044	0.045	0.032
ChessAV40	0.072	0.075	0.083	0.078	0.077
ChessBV40	0.088	0.095	0.109	0.114	0.101
ChessCV25	0.035	0.036	0.054	0.054	0.045
ChessDV50	0.068	0.064	0.083	0.089	0.076
HOAV35	0.028	0.028	0.038	0.039	0.033
HOEV50	0.057	0.055	0.084	0.085	0.070
HOBV20	0.017	0.016	0.040	0.040	0.028
HOCV40	0.105	0.106	0.093	0.100	0.101
HOFV20	0.031	0.031	0.080	0.080	0.056
HODV40	0.074	0.075	0.108	0.110	0.092

that developed VS can be used in controlled semi-active suspension mathematical models and its simulations. The performance testing of the application in a simulation environment is presented in the next subsection.

2.3. Performance evaluation of VS

The developed VS is integrated into a vehicle mathematical model with semi-active suspension and tested in real-time simulation. The vehicle mathematical model was developed in *IPG CarMaker* simulation platform, as it was described in Section 1. The *Skyhook* control strategy was realised in Matlab Simulink. The DNN was trained using *MATLAB* software (*https://www.mathworks.com/products/matlab.html*); the trained network was exported to *Simulink*. The *Simulink* model receives input data from *IPG CarMaker*, calculates and provides a controlled force that can vary in a specified range, and sends it back to simulation.

Real-life controllers use discrete signals from sensors; in this study. Therefore, 100 Hz sample frequency was selected, meaning SM and UM velocities used by the controller were taken every 10 ms. The NN was trained at the same 100 Hz frequency as well. VS performs in real-time because one iteration time is less than 10 ms.

It is not enough only to compare actual UM velocity value with VS data to test the proposed idea. The evaluation of change in comfort is required. As a comfort metric, the RMS value of vehicle SM accelerations in the vertical direction is commonly used in literature. In Table 4, the results of all 19 testing scenarios are provided. It can be seen that for six cases, the RMS of SM accelerations values is the same. For six tests, SM accelerations' RMS values are smaller than ones achieved using UM velocity directly. For seven tests, RMS increased when using VS. The maximal error is 17.9% for the test with road pits; the second worth result is 7% for the same type of road. The difference may be decreased by adding more data for training and validation datasets with this road type. In any case, even with the highest error of 17.9%, the absolute RMS difference is 0.07 m/s^2, which is less than a noticeable difference of 0.082 m/s^2, estimated for the rough road (Gräbe *et al.* 2020). It means that practically occupants will not feel the difference from changing the sensors.

Since the VS has been trained on simulation data, signal noise that is common for physical systems may affect its performance during real-life applications. Additional white noise was added to input signals that VS uses. The level of noise was up to 10% of maximal signal amplitude; it was added to 6 input signals: SM accelerations in 3 directions, pitch, yaw and roll. The rest signals used as input parameters do not contain noise in the actual system. In Figure 6, it can be seen how noise affects the input signal and the vertical velocity, which is received from VS. Developed sensor wasn't trained for this case even though it continues to perform stably.

In Table 4, the RMS of SM acceleration when noise is added is presented; it can be seen that the max difference is 0.05 m/s^2. Actual values are closer to actual sensor data, so it is proved that developed VS may perform with noisy data.

In Figure 7, SM acceleration in the vertical direction is presented as a function of time. Results were achieved using actual data from UM vertical velocity for suspension control directly and using data from VS. In Figure 7a representation of the scenario with trapezoidal road bumps is shown. During this test, the vehicle was moving at 50 km/h. The RMS of SM vertical acceleration is the same using actual data and the VS. However, analysing Figure 7a, a small difference in signals can be seen; the calculated RMSE is 0.165 m/s^2. The insignificant differences appear due to fluctuations in the longitudinal velocities of the vehicle. It appears as a mathematical model containing the driver model.

In Figure 7b, the road with pits scenario output is detailed. Differences caused by VS implementation are minimal – RMSE = 0.126 m/s^2. In this scenario, the RMSE value is lower than in the previous one; mostly, it is related to lower vehicle velocity as in a previous case. RMS values for both signals are the same (Table 4). In Figure 7c, the vehicle travels over the checkered pattern of trapezoidal road bumps. Contrary to the low RMS of SM difference between the sensors (Table 4), the calculated RMSE value is highest compared to the other two scenarios. The RMSE of 0.1986 m/s^2 was reached. Such a high RMSE value is related to unsymmetrical road disturbances, and more difficult to predict the scenario for the VS. The RMS difference for this case was 4.4%, and the absolute value was 0.01 m/s^2 is much less than the difference threshold.

Table 4. RMS values of SM accelerations

Test name	Actual sensor	VS	Difference [%]	VS with noise	Difference (with noise) [%]
	SM vertical acceleration RMS [m/s^2]	SM vertical acceleration RMS [m/s^2]		SM vertical acceleration RMS [m/s^2]	
TFAV50	0.48	0.48	0.0	0.47	2.1
TFBV25	0.44	0.45	–2.3	0.44	0.0
TFCV30	0.44	0.44	0.0	0.43	2.3
TFDV40	0.72	0.70	2.8	0.68	5.6
TFEV25	0.30	0.30	0.0	0.29	3.3
SINAV40	0.44	0.46	–4.5	0.43	2.3
SINBV40	1.23	1.28	–4.1	1.27	–3.3
SINCV30	0.81	0.85	–4.9	0.82	–1.2
SINDV25	0.39	0.38	2.6	0.39	0.0
ChessAV40	0.45	0.43	4.4	0.42	6.7
ChessBV40	0.51	0.50	2.0	0.50	2.0
ChessCV25	0.24	0.24	0.0	0.24	0.0
ChessDV50	0.71	0.70	1.4	0.69	2.8
HOAV35	0.43	0.43	0.0	0.42	2.3
HOEV50	1.09	1.06	2.8	1.04	4.6
HOBV20	0.30	0.30	0.0	0.30	0.0
HOCV40	0.39	0.46	–17.9	0.41	–5.1
HOFV20	1.00	1.07	–7.0	1.06	–6.0
HODV40	1.10	1.11	–0.9	1.08	1.8

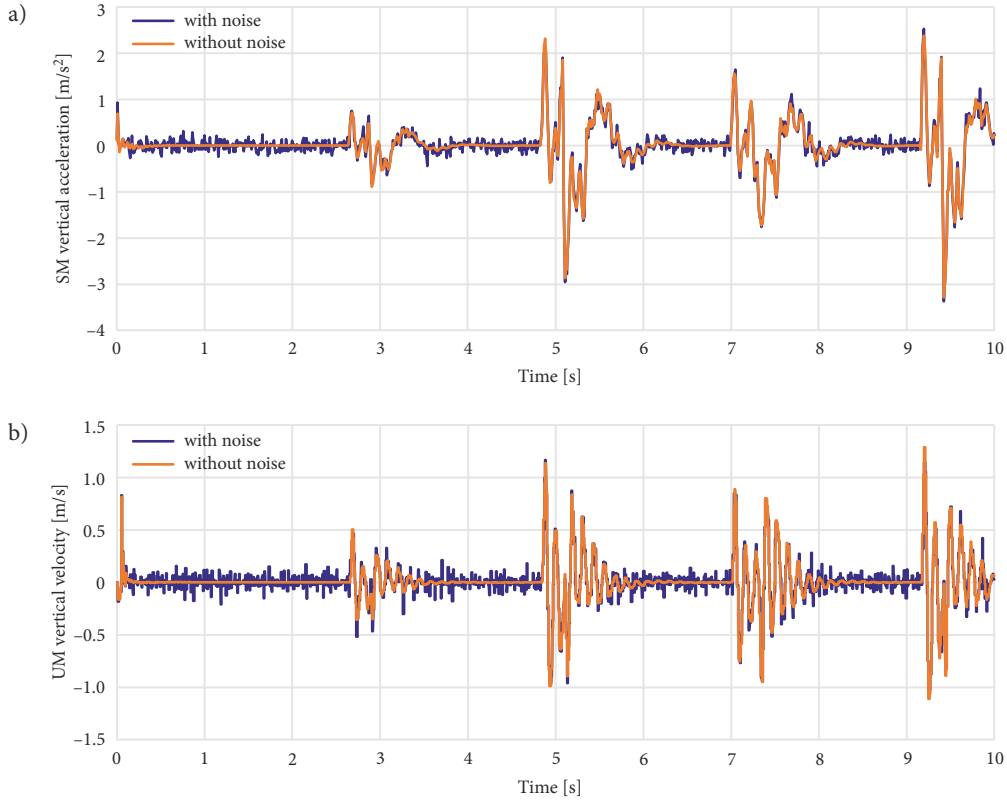

Figure 6. VS performance with noise: a – input with and without noise; b – output with and without noise

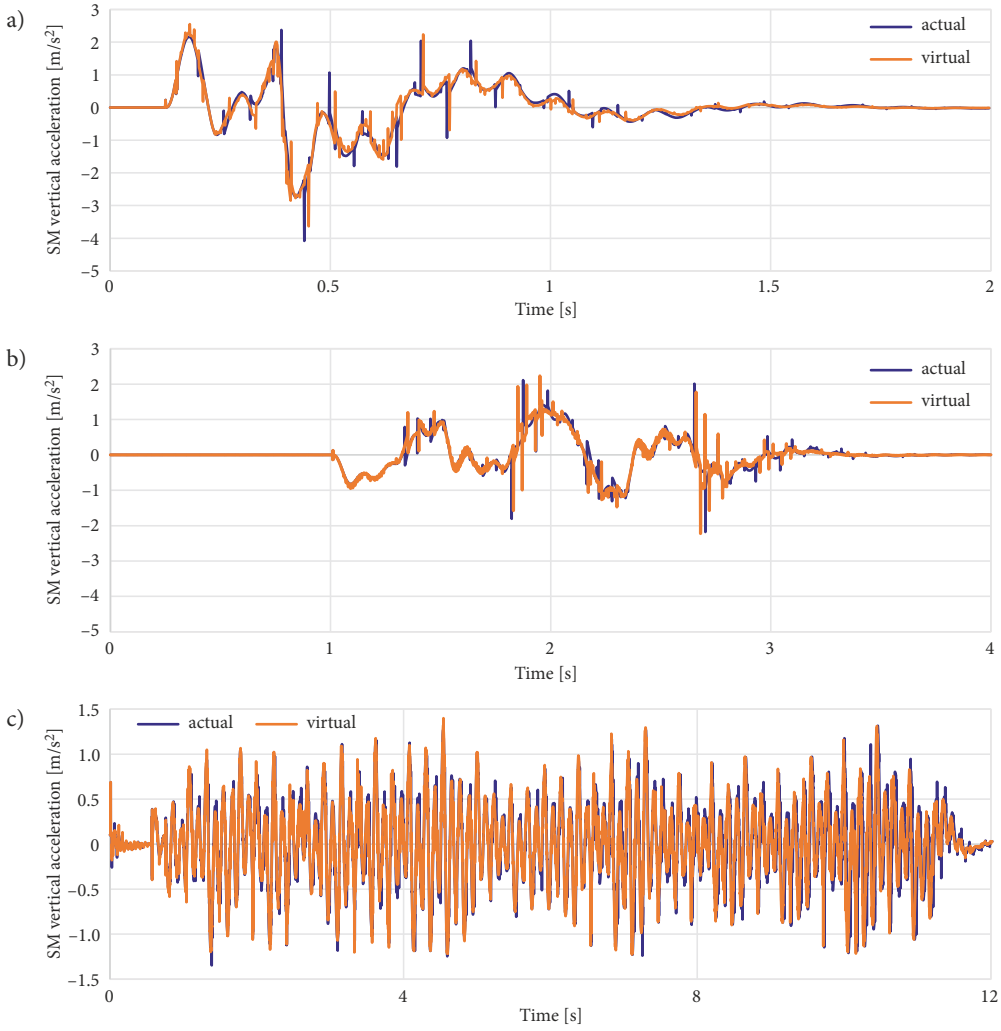

Figure 7. SM vertical acceleration using actual data from UM and data from VS: a – test TFAV50; b – test HOBV20; c – test ChessAV40

Conclusions

Previously NN-based data-driven sensors were developed for road roughness estimation and for SM vertical velocity estimation on vehicles with passive suspension only. In this paper, the hypothesis is that changing the physical UM vertical velocity sensor with NN-based VS will have minimal effect on comfort. To test it, NN-based data-driven VSs impact on comfort metric RMS of SM was analysed when used with *Skyhook* control algorithm and compared to direct measurements acquired from simulation. VS were integrated and tested on a simulation platform using a high-fidelity SUV model for the first time.

The 7 layers NN-model called 1D CNN was used for the VS. That VS uses 14 signals as inputs and provides real-valued outputs that estimate output signals. The output is a vector of 4 values; each corresponds to the estimated UM vertical velocity. These UMs correspond to FL, FR, RL, and RR wheels. VS runs in less than 10 ms, that is the period of suspension control algorithms set for used models. That allows real-time running of VS.

As data-driven VS requires data for training, an original and extensive dataset covering 95 scenarios has been developed and divided into training, validation and testing parts. There are four groups of tests in datasets: (1) various trapezoidal road bumps; (2) sinusoidal road profiles; (3) trapezoidal road bumps placed in a checkered pattern; (4) road profiles with pits. Scenarios include a variety of geometrical parameters and driving speeds in a range from 10 to 60 km/h. Safe driving cannot be ensured by moving faster in selected scenarios; therefore, there is no need to investigate higher speeds.

Presented research proves that DNN-based data-driven sensor performs well in a vehicle equipped with semi-active suspension. As a comfort metric RMS value of SM acceleration was used in this research. Solution effectiveness was tested on 19 scenarios; for the majority of the cases (63%), the comfort level was the same as using data from SM directly or even slightly better. For 37% of the cases, RMS values increased. However, the maximal RMS difference was 0.07 m/s^2, while the difference threshold for the same vehicle driving on a rough surface is 0.08 m/s^2

(such a difference will feel 50% of the occupants). It means that practically occupants will not feel the difference from changing the sensors. The results achieved in real-time simulation show a possibility of replacing physical sensors with virtual ones. Signal noise that is common for physical systems may affect their performance during real-life applications. The noise was added to signals that VS uses as input. It was found that VS output does not change significantly, and the developed sensor may perform under such disturbances. In future, the development of VS for UM vertical velocity using experimental data recorded on proving grounds from the vehicle and such VS testing in real-time on a real vehicle is planned.

Funding

This research was funded from the European Union Horizon 2020 Framework Program, Marie Skłodowska-Curie actions, under Grant Agreement No 872907.

Author contributions

Conceptualisation – *Viktor Skrickij*, *Eldar Šabanovič* and *Paulius Kojis*.

Mathematical modelling – *Paulius Kojis* and *Eldar Šabanovič*.

Formal analysis – *Viktor Skrickij*, *Paulius Kojis* and *Eldar Šabanovič*.

Data curation – *Eldar Šabanovič* and *Paulius Kojis*.

Writing (original draft) – *Viktor Skrickij*, *Paulius Kojis* and *Eldar Šabanovič*.

All authors have read and agreed to the published version of the manuscript.

Disclosure statement

The authors declare no conflict of interest.

References

Acosta, M.; Kanarachos, S.; Fitzpatrick, M. E. 2017. A virtual sensor for integral tire force estimation using tire model-less approaches and adaptive unscented Kalman filter, in *Proceedings of the 14th International Conference on Informatics in Control, Automation and Robotics*, 26–27 July 2017, Madrid, Spain, 1: 386–397. https://doi.org/10.5220/0006394103860397

Ahamed, P. S. S.; Duraiswamy, P. 2019. Virtual sensing active noise control system with 2d microphone array for automotive applications, in *2019 6th International Conference on Signal Processing and Integrated Networks* (*SPIN*), 7–8 March 2019, Noida, India, 151–155. https://doi.org/10.1109/spin.2019.8711608

Al-Ashmori, M.; Wang, X. 2020. A systematic literature review of various control techniques for active seat suspension systems, *Applied Sciences* 10(3): 1148. https://doi.org/10.3390/app10031148

Cao, D.; Song, X.; Ahmadian, M. 2011. Editors' perspectives: road vehicle suspension design, dynamics, and control, *Vehicle System Dynamics: International Journal of Vehicle Mechanics and Mobility* 49(1–2): 3–28. https://doi.org/10.1080/00423114.2010.532223

Choi, Y.; Yoon, S. 2020. Virtual sensor-assisted *in situ* sensor calibration in operational HVAC systems, *Building and Environment* 181: 107079. https://doi.org/10.1016/j.buildenv.2020.107079

Fares, A.; Bani Younes, A. 2020. Online reinforcement learning-based control of an active suspension system using the actor critic approach, *Applied Sciences* 10(22): 8060. https://doi.org/10.3390/app10228060

Floreán-Aquino, K. H.; Arias-Montiel, M.; Linares-Flores, J.; Mendoza-Larios, J. G.; Cabrera-Amado, Á. 2021. Modern semi-active control schemes for a suspension with MR actuator for vibration attenuation, *Actuators* 10(2): 22. https://doi.org/10.3390/act10020022

Ghoniem, M.; Awad, T.; Mokhiamar, O. 2020. Control of a new low-cost semi-active vehicle suspension system using artificial neural networks, *Alexandria Engineering Journal* 59(5): 4013–4025. https://doi.org/10.1016/j.aej.2020.07.007

Gräbe, R. P.; Kat, C.-J.; Van Staden, P. J.; Els, P. S. 2020. Difference thresholds for a vehicle on a 4-poster test rig, *Applied Ergonomics* 87: 103115. https://doi.org/10.1016/j.apergo.2020.103115

Jain, S.; Saboo, S.; Pruncu, C. I.; Unune, D. R. 2020. Performance investigation of integrated model of quarter car semi-active seat suspension with human model, *Applied Sciences* 10(9): 3185. https://doi.org/10.3390/app10093185

Jeong, K.; Choi, S. B. 2019. Vehicle suspension relative velocity estimation using a single 6-D IMU sensor, *IEEE Transactions on Vehicular Technology* 68(8): 7309–7318. https://doi.org/10.1109/tvt.2019.2920876

Jiang, H.; Wang, C.; Li, Z.; Liu, C. 2021. Hybrid model predictive control of semiactive suspension in electric vehicle with hub-motor, *Applied Sciences* 11(1): 382. https://doi.org/10.3390/app11010382

Jierula, A.; Wang, S.; Oh, T.-M.; Wang, P. 2021. Study on accuracy metrics for evaluating the predictions of damage locations in deep piles using artificial neural networks with acoustic emission data, *Applied Sciences* 11(5): 2314. https://doi.org/10.3390/app11052314

Kahraman, K.; Emirler, M. T.; Centürk, M.; Güvenç, B. A.; Güvenç, L.; Efendioğlu, B. 2010. Estimation of vehicle yaw rate using a virtual sensor with a speed scheduled observer, *IFAC Proceedings Volumes* 43(7): 632–637. https://doi.org/10.3182/20100712-3-de-2013.00043

Khatibisepehr, S.; Huang, B.; Khare, S. 2013. Design of inferential sensors in the process industry: a review of Bayesian methods, *Journal of Process Control* 23(10): 1575–1596. https://doi.org/10.1016/j.jprocont.2013.05.007

Kim, G.; Lee, S. Y.; Oh, J.-S.; Lee, S. 2021. Deep learning-based estimation of the unknown road profile and state variables for the vehicle suspension system, *IEEE Access* 9: 13878–13890. https://doi.org/10.1109/access.2021.3051619

Koch, G. P. A. 2011. *Adaptive Control of Mechatronic Vehicle Suspension Systems*. PhD Dissertation. Technical University of Munich, Germany. 250 p. Available from Internet: http://mediatum.ub.tum.de/doc/1002476/document.pdf

Konoiko, A.; Kadhem, A.; Saiful, I.; Ghorbanian, N.; Zweiri, Y.; Sahinkaya, M. N. 2019. Deep learning framework for controlling an active suspension system, *Journal of Vibration and Control* 25(17): 2316–2329. https://doi.org/10.1177/1077546319853070

LAKD. 2010. *Inžinerinių saugaus eismo priemonių projektavimo ir naudojimo rekomendacijos R ISEP 10*. Lietuvos automobilių kelių direkcija (LAKD) prie Susisiekimo ministerijos, Vilnius, 127 p. Available from Internet: https://e-seimas.lrs.lt/portal/legalAct/lt/TAD/TAIS.375622

Li, H.; Yu, D.; Braun, J. E. 2011. A review of virtual sensing technology and application in building systems, *HVAC&R Research 17*(5): 619–645.

Liu, C.; Chen, L.; Yang, X.; Zhang, X.; Yang, Y. 2019. General theory of skyhook control and its application to semi-active suspension control strategy design, *IEEE Access* 7: 101552–101560. https://doi.org/10.1109/access.2019.2930567

Marques, T.; Reynoso-Meza, G. 2020. Applications of multi-objective optimisation for PID-like controller tuning: a 2015–2019 review and analysis, *IFAC-PapersOnLine* 53(2): 7933–7940. https://doi.org/10.1016/j.ifacol.2020.12.2140

Martin, D.; Kühl, N.; Satzger, G. 2021. Virtual sensors, *Business & Information Systems Engineering* 63(3): 315–323. https://doi.org/10.1007/s12599-021-00689-w

Mattera, C. G.; Quevedo, J.; Escobet, T.; Shaker, H. R.; Jradi, M. 2018. A method for fault detection and diagnostics in ventilation units using virtual sensors, *Sensors* 18(11): 3931. https://doi.org/10.3390/s18113931

Milanese, M.; Ruiz, F.; Taragna, M. 2007. Linear virtual sensors for vertical dynamics of vehicles with controlled suspensions, in *2007 European Control Conference* (*ECC*), 2–5 July 2007, Kos, Greece, 1257–1263. https://doi.org/10.23919/ecc.2007.7068662

Mozaffari, A.; Chenouri, S.; Qin, Y.; Khajepour, A. 2019. Learning-based vehicle suspension controller design: a review of the state-of-the-art and future research potentials, *eTransportation* 2: 100024. https://doi.org/10.1016/j.etran.2019.100024

Omrane, I.; Etien, E.; Dib, W.; Bachelier, O. 2015. Modeling and simulation of soft sensor design for real-time speed and position estimation of PMSM, *ISA Transactions* 57: 329–339. https://doi.org/10.1016/j.isatra.2014.06.004

Pellegrini, E. 2012. *Model-Based Damper Control for Semi-Active Suspension Systems*. PhD Dissertation. Technical University of Munich, Germany. 196 p. Available from Internet: https://mediatum.ub.tum.de/doc/1113007/document.pdf

Pletschen, N.; Badur, P. 2014. Nonlinear state estimation in suspension control based on Takagi–Sugeno model, *IFAC Proceedings Volumes* 47(3): 11231–11237. https://doi.org/10.3182/20140824-6-za-1003.02500

Qin, Y.; He, C.; Ding, P.; Dong, M.; Huang, Y. 2018. Suspension hybrid control for in-wheel motor driven electric vehicle with dynamic vibration absorbing structures, *IFAC-PapersOnLine* 51(31): 973–978. https://doi.org/10.1016/j.ifacol.2018.10.054

Sathishkumar, P.; Wang, R.; Yang, L.; Thiyagarajan, J. 2021. Energy harvesting approach to utilize the dissipated energy during hydraulic active suspension operation with comfort oriented control scheme, *Energy* 224: 120124. https://doi.org/10.1016/j.energy.2021.120124

Savaresi, D.; Favalli, F.; Formentin, S.; Savaresi, S. M. 2019. Online damping estimation in road vehicle semi-active suspension systems, *IFAC-PapersOnLine* 52(5): 679–684. https://doi.org/10.1016/j.ifacol.2019.09.108

Savaresi, S. M.; Poussot-Vassal, C.; Spelta, C.; Sename, O.; Dugard, L. 2010. Classical control for semi-active suspension system, in *Semi-Active Suspension Control Design for Vehicles*, Chapter 6, 107–120. https://doi.org/10.1016/b978-0-08-096678-6.00006-7

Savitski, D.; Schleinin, D.; Ivanov, V.; Augsburg, K. 2017. Sliding mode approach in semi-active suspension control, in A. Ferrara (Ed.). *Sliding Mode Control of Vehicle Dynamics*, 191–228. https://doi.org/10.1049/PBTR005E_ch6

Skrickij, V.; Savitski, D.; Ivanov, V.; Skačkauskas, P. 2018. Investigation of cavitation process in monotube shock absorber, *International Journal of Automotive Technology* 19(5): 801–810. https://doi.org/10.1007/s12239-018-0077-1

Soliman, A. M. A.; Kaldas, M. M. S. 2021. Semi-active suspension systems from research to mass-market – a review, *Journal of Low Frequency Noise, Vibration and Active Control* 40(2): 1005–1023. https://doi.org/10.1177/1461348419876392

Son, T. D.; Bhave, A.; Vandermeulen, W.; Geluk, T.; Worm, M.; Van der Auweraer, H. 2020. *Model-Based and Data-Driven Learning Control for Safety and Comfort for Autonomous Driving*. White Paper. Siemens, Plano, TX, US. 16 p. https://doi.org/10.13140/RG.2.2.13850.88003

Sun, S.-B.; He, Y.-Y.; Zhou, S.-D.; Yue, Z.-J. 2017. A data-driven response virtual sensor technique with partial vibration measurements using convolutional neural network, *Sensors* 17(12): 2888. https://doi.org/10.3390/s17122888

Šabanovič, E.; Kojis, P.; Šukevičius, Š.; Shyrokau, B.; Ivanov, V.; Dhaens, M.; Skrickij, V. 2021. Feasibility of a neural network-based virtual sensor for vehicle unsprung mass relative velocity estimation, *Sensors* 21(21): 7139. https://doi.org/10.3390/s21217139

Theunissen, J.; Tota, A.; Gruber, P.; Dhaens, M.; Sorniotti, A. 2021. Preview-based techniques for vehicle suspension control: a state-of-the-art review, *Annual Reviews in Control* 51: 206–235. https://doi.org/10.1016/j.arcontrol.2021.03.010

Vandersmissen, B.; Six, K.; Reybrouck, K. 2012. ACOCAR: ultimate comfort and safety through the energy-efficient active damping system of Tenneco, in *21st Aachen Colloquium Automobile and Engine Technology 2012*, 8–10 October 2012, Aachen, Germany. 15 p. Available from Internet: https://www.aachener-kolloquium.de/images/tagungsunterlagen/2012_21._ACK/C3.3_Reybrouck_Tenneco.pdf

Viehweger, M.; Vaseur, C.; Van Aalst, S.; Acosta, M.; Regolin, E.; Alatorre, A.; Desmet, W.; Naets, F.; Ivanov, V.; Ferrara, A.; Victorino, A. 2021. Vehicle state and tyre force estimation: demonstrations and guidelines, *Vehicle System Dynamics: International Journal of Vehicle Mechanics and Mobility* 59(5): 675–702. https://doi.org/10.1080/00423114.2020.1714672

Yatak, M. Ö., Şahin, F. 2021. Ride comfort-road holding trade-off improvement of full vehicle active suspension system by interval type-2 fuzzy control, *Engineering Science and Technology, an International Journal* 24(1): 259–270. https://doi.org/10.1016/j.jestch.2020.10.006

Zaharia, C.; Clenci, A. 2013. Study on virtual sensors and their automotive applications, *Scientific Bulletin – Automotive Series* (23): 68–74. Available from Internet: https://automotive.upit.ro/index_files/2013/2013_A_8_.pdf

Zheng, Y.; Shyrokau, B.; Keviczky, T.; Al Sakka M.; Dhaens, M. 2021. Curve tilting with nonlinear model predictive control for enhancing motion comfort, *IEEE Transactions on Control Systems Technology* (Early Access): 1–12. https://doi.org/10.1109/TCST.2021.3113037

Zhou, C.; Liu, X.; Chen, W.; Xu, F.; Cao, B. 2018. Optimal sliding mode control for an active suspension system based on a genetic algorithm, *Algorithms* 11(12): 205. https://doi.org/10.3390/a11120205